An Efficient Technique for the Design of an Arrayed-Waveguide Grating With Flat Spectral Response

Thomas Kamalakis and Thomas Sphicopoulos, *Member, IEEE*

***Abstract*—The spectral response of the arrayed-waveguide grating (AWG) plays an important role in optical networks. Ideally, the grating should have a rectangular transfer function to reduce the need for accurate wavelength control and achieve low crosstalk. In this paper, a new technique for designing an AWG with flat spectral response is presented. The problem of the optimization of the transfer function is reduced to that of adjusting the arrayed waveguide lengths and their relative positions on the edge of the free propagating regions in order to minimize a certain error function. As a result, the waveguide lengths and their positions are determined using a rigorous mathematical procedure. The resultant transfer function is flat with low sidelobes.**

***Index Terms*—Gratings, integrated optics, optical filters, optical planar waveguide components, waveguide filters, wavelength division multiplexing (WDM).**

I. Introduction

THE PERFORMANCE of wavelength division multiplexing (WDM) optical networks [1] greatly depends on the spectral characteristics of their components. One key component of WDM networks is the arrayed waveguide grating (AWG) [2], which can serve as a wavelength router, multiplexer, and demultiplexer. In order to allow the concatenation of many such devices and reduce the need for accurate wavelength control, their filter response must approximate a rectangular function. Various techniques [3]–[7] have been proposed in order to broaden and flatten the transfer function of an AWG. In this paper, a rigorous mathematical technique for designing the transfer function of an AWG is presented. This technique, resulting in the modification of the lengths of the grating waveguides, is an extension of the deterministic tapering technique used in the design of antenna arrays [8]. In fact, since the spectral transfer function of an AWG and the spatial transfer function of an antenna array are alike, the two problems are similar. The deterministic tapering method consists of finding the optimum lengths of the grating waveguides in order to produce a transfer function that approximates a given ideal function. It is based on a strict mathematical formalism that leads to the minimization of an error function, thus avoiding the use of empirical rules. In order to achieve the same passband for all output ports, the positions of the grating waveguides on the edge of the free propagating regions (FPRs) are also adjusted. The 3-dB bandwidth of the resultant transfer function can assume different values, according to the design requirements, by varying the lengths and the positions of the waveguides, without changing their number. The sidelobe levels are low, resulting in a reduced crosstalk. The losses introduced by using this technique, compared to those introduced using other techniques [7], are less important. Because of the design procedure, the chromatic dispersion of the filter should be negligible.

The paper is organized as follows. In Section II, the theoretical background on which the extension of the deterministic tapering technique is based is given. In Section III, the results obtained by this technique are presented and commented; in Section IV, they are compared with those of other proposed methods altering the grating arms as well.

II. Theoretical Analysis

The transfer function between the central input port of an AWG demultiplexer and its output port located at distance y_{qo} from its central output port is given by [10]

$$H_q(f) = \sum_{m=-P}^{P} C_m \exp(j2\pi t_m f - j\kappa y_m y_{qo} f) \qquad (1)$$

where f is the frequency of the optical spectrum and C_m the optical power of the mth grating waveguide normalized to the total power (C_m is a dimensionless quantity), located at position y_m from the central grating waveguide (see Fig. 1). Equation (1) can be derived by assuming that the incident mode of the waveguides can be approximated by a Gaussian distribution $\exp(-y^2/2\sigma^2)$. It is also assumed, for simplicity, that the efficiency is the same for all output ports of the AWG. The total number of waveguides is equal to $2P+1$ and the values of the parameters t_m are given by

$$t_m = nL_m/c \qquad (2)$$

where n is the effective refractive index of the grating, c the velocity of light in vacuum, and L_m is the the difference between the length of the mth waveguide and the length of the central waveguide ($L_0 = 0$). Finally, the constant κ is given by

$$\kappa = \frac{2\pi n}{cR} \qquad (3)$$

Manuscript received January 11, 2001; revised June 18, 2001.

The authors are with the Department of Informatics and Telecommunications of the University of Athens, Panepistimiopolis, Athens GR-157 84, Greece (e-mail: thkam@di.uoa.gr; thomas@di.uoa.gz).

Publisher Item Identifier S 0733-8724(01)09637-2.

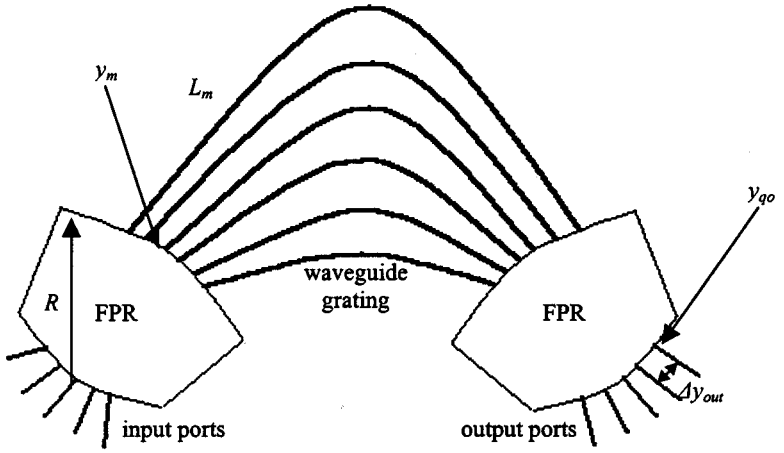

Fig. 1. A conventional $N \times N$ AWG.

where R is the radius of the FPRs. It is assumed that the effective refractive indexes of the FPR and the grating are approximately equal due to the weak guidance approximation [9].

Assuming the Gaussian approximation [9] for the waveguide modes, the coefficients C_m are found to obey an exponential law given by

$$C_m = C_0 \exp(-a^2 y_m^2) \tag{4}$$

where a is given by

$$a = \frac{2\pi n \sigma}{cR} f_0. \tag{5}$$

In (5), σ is the variance of the Gaussian distribution with which the fundamental waveguide mode profile of the grating is approximated and f_0 is the central frequency.

In a conventional AWG, shown in Fig. 1, the values of t_m are given by

$$t_m = \frac{m}{\text{FSR}} \tag{6}$$

where FSR is the free spectral range of the AWG and is related to the central frequency f_0 by

$$\text{FSR} = \frac{f_0}{N} \tag{7}$$

with N being the order of the grating. The transfer function of a conventional AWG has a Gaussian shape and very low sidelobes.

In the proposed design, t_m are unknown quantities and their optimal values are determined so that the transfer function $H(f)$ between the central input waveguide and the central output waveguide, obtained from (1) by setting $y_{qo} = 0$

$$H(f) = \sum_{m=-P}^{P} C_m \exp(j2\pi t_m f) \tag{8}$$

approximates a rectangular function

$$H_0(f) = \begin{cases} 1, & |f - f_0| \le \Delta f_p/2 \\ 0, & \text{otherwise} \end{cases} \tag{9}$$

where Δf_p is the width of the rectangular function. Toward this end, an extension of the deterministic tapering method [8] is employed. First, it is required that

$$t_m = i_m/(2f_0) \tag{10}$$

where the i_m are integers. The analysis is facilitated by setting $F = f - f_0$ (F is the frequency measured from the central frequency f_0). Substituting (10) into(8), the transfer function $H(F)$ can be written as

$$H(F) = \sum_{m=-P}^{P} C_m (-1)^{a_m} \exp(j2\pi t_m F) \tag{11}$$

where $\exp(j\pi i_m)$ has been substituted by $(-1)^{a_m}$ and the exponents a_m are determined by

$$a_m = \text{mod}(i_m, 2). \tag{12}$$

In (12), $\text{mod}(x, y)$ represents the modulus of the division of x by y. The exponents a_m determine the sign of each term of the sum in (11). The objective is to make (11) as close as possible to $H_0(F)$

It is required that

$$C_m = C_{-m} \qquad t_m = -t_{-m} \qquad a_m = a_{-m} \tag{13}$$

which ensures that $H(F)$ is real

$$H(F) = C_0 + 2\sum_{m=1}^{P} (-1)^{a_m} C_m \cos(2\pi t_m F). \tag{14}$$

The first constraint in (13) is implied by (4) when the waveguides are positioned symmetrically with respect to the central waveguide, and dictates that the optical power of the grating waveguides is also symmetric. The physical significance of the second constraint in (13) is that the distribution L_m of the differences of the waveguide lengths from the length of the central waveguide in the array is antisymmetric, whereas the third constraint means that if the phase of the signal in the mth waveguide is rotated by π radians ($a_m = 1$), then the phase of the signal in the waveguide found in the symmetric position with respect to the central waveguide is also rotated by π ($a_{-m} = 1$).

Following the deterministic tapering method, $H(F)$ and $H_0(F)$ are expressed in terms of their Fourier transforms $h(t)$ and $h_0(t)$, respectively

$$H(F) = \int_{-\infty}^{+\infty} h(t)\cos(2\pi Ft)\,dt \tag{15}$$

$$H_0(F) = \int_{-\infty}^{+\infty} h_0(t)\cos(2\pi Ft)\,dt \tag{16}$$

where

$$h(t) = C_0\delta(t) + \sum_{m=-P}^{P} C_m(-1)^{a_m}\delta(t-t_m) \tag{17}$$

$$h_0(t) = \Delta f_p \operatorname{sinc}(\Delta f_p t). \tag{18}$$

$\delta(t)$ denotes the Dirac function (measured in s^{-1}), and sinc denotes the sinc function. Using (15) and (16), the symmetry of $h(t)$ and $h_0(t)$ and integrating by parts, it can be shown that

$$\frac{H(F)-H_0(F)}{2\pi F} = \int_{-\infty}^{+\infty}[A(t)-A_0(t)]\sin(2\pi Ft)\,dt \tag{19}$$

where

$$A(t) = \int_0^t h(\tau)\,d\tau = \sum_{t_m \le t} C_m(-1)^{a_m} \tag{20}$$

$$A_0(t) = \int_0^t h_0(\tau)\,d\tau = \int_0^t \Delta f_p \operatorname{sinc}(\Delta f_p \tau)\,d\tau. \tag{21}$$

Both $A(t)$ and $A_0(t)$ are dimensionless. Applying Parseval's theorem [11] to (19), the following result is obtained:

$$E = \frac{1}{4\pi^2}\int_{-\infty}^{+\infty}\left|\frac{H(F)-H_0(F)}{F}\right|^2 dF = \int_{-\infty}^{+\infty}|A(t)-A_0(t)|^2\,dt = 2\int_0^{+\infty}|A(t)-A_0(t)|^2\,dt \tag{22}$$

where E is the error function between $H(F)$ and $H_0(F)$. This last result suggests that, in order to match $H(F)$ to $H_0(F)$, t_m must be chosen to minimize the difference between $A(t)$ and $A_0(t)$. Differentiating (22) with respect to t_m and setting the result of the differentiation equal to zero, the following solutions for t_m are obtained:

$$2A_0(t_m) = \sum_{k=0}^{m-1}(-1)^{a_k}C_k + 2(-1)^{a_m}C_m, \quad m = 0,1,\ldots P. \tag{23}$$

To solve (23), the values of C_m must be determined using (4). In order to ensure that the transfer functions of the other output waveguides also match a rectangular function, the positions y_m of the waveguides must be set proportional to t_m

$$y_m = ut_m \tag{24}$$

where u is given by

$$u = \frac{cR\Delta f_{\text{ch}}}{f_0 n \Delta y_{\text{out}}} \tag{25}$$

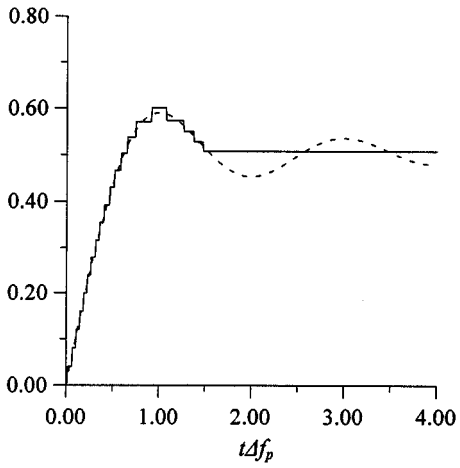

Fig. 2. The functions $A_0(t\Delta f_p)$ (drawn with dotted lines) and $A(t\Delta f_p)$ (drawn with solid lines). The initial step size is chosen $C_0 = 0.05$, the attenuation constant b is equal to 0.05 THz, and $\Delta f_p = 0.16$ THz.

with Δf_{ch} being the adjacent channel frequency spacing and Δy_{out} being the center-to-center separation of the adjacent output waveguides. This technique is known as double chirping [10]. Substituting (24) and (25) into (1), $H_q(f) = H(f - q\Delta f_{\text{ch}})$ is obtained, $H(f)$ being the transfer function of the central output waveguide and $H_q(f)$ being the transfer function of the qth waveguide. By substituting (24) and (25) into (4), and using (5), the following relation between C_m and t_m is obtained:

$$C_m = C_0\exp(-b^2t_m^2) \tag{26}$$

where the attenuation constant b is given by

$$b = au = \frac{2\pi\sigma\Delta f_{\text{ch}}}{\Delta y_{\text{out}}}. \tag{27}$$

Equation (23) can now be solved numerically in order to determine the values of t_m. The solution is divided in P steps and, at the end of step m, a solution for t_m is obtained by solving recursively the following equations:

$$t_0 = 0$$

$$A_0(t_1) = C_0(-1)^{a_1}\exp(-b^2t_1^2)/2$$

$$A_0(t_i) = C_0\sum_{k=0}^{i-1}(-1)^{a_k}\exp(-b^2t_k^2) + C_0\frac{(-1)^{a_i}\exp(-b^2t_i^2)}{2}$$

$$A_0(t_p) = C_0\sum_{k=0}^{P-1}(-1)^{a_k}\exp(-b^2t_k^2) + C_0\frac{(-1)^{a_P}\exp(-b^2t_P^2)}{2}.$$

The exponents a_m, which have been defined in (12), are determined by the solution algorithm so that $A(t)$ and $A_0(t)$ come as close as possible. An example is illustrated in Fig. 2, where $A_0(t\Delta f_p)$ and $A(t\Delta f_p)$ are plotted. For $t\Delta f_p \in (0,1)$, $A_0(t\Delta f_p)$ is increasing with t and steps must be added ($a_m = 0$) to $A(t\Delta f_p)$ in order to follow A_0. For $t\Delta f_p \in (1,2)$, where $A_0(t\Delta f_p)$ is decreasing, steps must be subtracted ($a_m = 1$) from $A(t\Delta f_p)$. The points where $A(t\Delta f_p)$ and $A_0(t\Delta f_p)$ intersect are equal to $t_m\Delta f_p$. Because there is a finite number P of C_m, $A(t\Delta f_p)$ is set constant for

$t\Delta f_p > t_P \Delta f_p$ (t_P corresponds to the last waveguide). The value of t_P is determined by the attenuation constant b, the initial step C_0, and the number of waveguides $(2P+1)$.

III. Design Results

It becomes evident that the three major factors that determine the design are: 1) the number of grating waveguides to be used; 2) the initial step size, equal to C_0; and 3) the damping rate of the steps C_m determined by the constant b in (26). Using this method, the objective is the transfer function $H(f)$ to approximate $H_0(f)$. In order to measure the performance of the method, the flatness of the 3-dB bandwidth and the sidelobe level must be calculated. The sidelobe level is related to the crosstalk between the various channels.

To measure the flatness of the transfer function, the ripple $\sigma^2_{3\,\mathrm{dB}}$ [7] is calculated within the 3-dB bandwidth using

$$\sigma^2_{3\,\mathrm{dB}} = \frac{1}{\Delta f_{3\,\mathrm{dB}} \bar{H}^2} \int_{-\Delta f_{3\,\mathrm{dB}}/2}^{\Delta f_{3\,\mathrm{dB}}/2} |H(F) - \bar{H}|^2 \, dF \qquad (28)$$

where $\bar{H}$ denotes the average amplitude of $H(F)$ in the 3-dB bandwidth $(\Delta f_{3\,\mathrm{dB}})$

$$\bar{H} = \frac{1}{\Delta f_{3\,\mathrm{dB}}} \int_{-\Delta f_{3\,\mathrm{dB}}/2}^{\Delta f_{3\,\mathrm{dB}}/2} H(F) \, dF. \qquad (29)$$

In (14), some terms appear with negative signs. It is expected that the tapered design introduces some losses L_{dB} due to these negative terms given by

$$L_{\mathrm{dB}} = 20 \log_{10} \left(H(0) / H^p_{\max} \right) \qquad (30)$$

with

$$H^p_{\max} = \sum_{m=-P}^{P} C_m \qquad (31)$$

and

$$H(0) = \sum_{m=-P}^{P} (-1)^{a_m} C_m. \qquad (32)$$

Also, since the waveguides are not equidistant some insertion loss will be added. The total losses due to the tapered design could be made less than -3 dB.

The transfer function $H(F)$ is real because the t_m are antisymmetric, as required by (13); the transfer function is also expected to match a positive rectangular transfer function $H_0(F)$. As a consequence, the transfer function $H(F)$ will be positive within its main lobe and the dispersion of the filter should be negligible because the group delay, determined by the derivative of the phase, will be equal to zero.

In order to illustrate the effect of the various parameters, a tapered AWG is designed with eight channels equally spaced by $\Delta f_{\mathrm{ch}} = 0.2$ THz. The 3-dB bandwidth of the transfer function is required to be approximately $\Delta f_p = 0.16$ THz. The central channel is located at $\lambda_0 = 1.55$ μm ($f_0 = 193.55$ THz). P is chosen equal to 40, corresponding to a total of $M = 2P + 1 = 81$ waveguides in the grating.

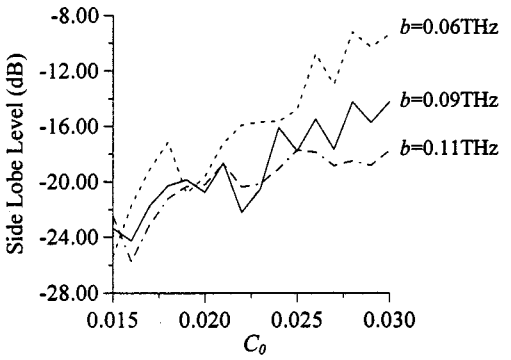

Fig. 3. Dependence of the sidelobe level from the initial step C_0 for different attenuation constants b.

A. Sidelobe Level and 3-dB Ripple

Fig. 3 describes, for different values of the attenuation coefficient b, the behavior of the sidelobe level with respect to the magnitude of the step C_0 (corresponding to $t = t_0 = 0$), from which all C_m depend [see (26)]. It is evident that the sidelobe level is strongly dependent on these quantities. When the step C_0 is too small, the main lobe of the transfer function of the tapered AWG is found to resemble that of the conventional AWG. As the step C_0 increases, the tapered transfer function attempts to approximate $H_0(f)$, but the sidelobes are higher. Increasing C_0 results in larger steps C_m and, for a given P, the function $A(t\Delta f_p)$ follows $A_0(t\Delta f_p)$ in a larger interval (see Fig. 2). The attenuation coefficient b is important because it determines how the function $A(t\Delta f_p)$ approximates $A_0(t\Delta f_p)$ in the region $t\Delta f_p > 1$ where $A_0(t\Delta f_p)$ oscillates. From Fig. 2, it is deduced that the steps C_m (depending on b) of $A(t)$ in this region must be smaller than those in the region $t\Delta f_p < 1$ in order to follow these oscillations. However, the steps should not be made too small because, in this case, many more steps would be required in order to follow $A_0(t\Delta f_p)$ in the region $t\Delta f_p \in [1, 2]$. Consequently, b should not be too large.

The above remarks are illustrated in Fig. 4, where the normalized tapered transfer function is plotted for a value of $b = 0.09$ THz and for three different values of C_0. In Fig. 4(a), $(C_0 = 0.016)$, the sidelobes are low (-24.2 dB), and the shape of the transfer function resembles that of a conventional AWG, but has higher sidelobes. The increase in sidelobe level is attributed to three reasons. First, as shown in Fig. 2, the function $A(t\Delta f_p)$ approximates $A_0(t\Delta f_p)$ in a finite interval of $t\Delta f_p$ only. Second, $A(t\Delta f_p)$ is equal to $A_0(t\Delta f_p)$ only on $t\Delta f_p = t_m \Delta f_p$. The third reason is the fact that the integrand in (22) has an $1/F^2$ frequency dependence. This means that $H_0(F)$ approximates $H(F)$ near $F = 0$, but as F becomes larger, there can be some difference between them. In Fig. 4(b), $(C_0 = 0.02)$ and the sidelobes are higher (-20.3 dB), but the flattest 3-dB bandwidth is achieved. Fig. 4(c) presents a compromise between the previous cases with sidelobes not exceeding -23 dB. In Fig. 4(d), the functions $A(t\Delta f_p)$ and $A_0(t\Delta f_p)$ in each case are shown. As the interval in which $A(t\Delta f_p)$ follows $A_0(t\Delta f_p)$ increases, $H(f)$ tends to become more rectangular. However, as the flatness of $H(f)$ becomes better, its sidelobes increase. For the cases a, b, and c of Fig. 4, the ripple is 0.0370, 0.0204, and 0.0266, respectively. Fig. 5 depicts the variation of

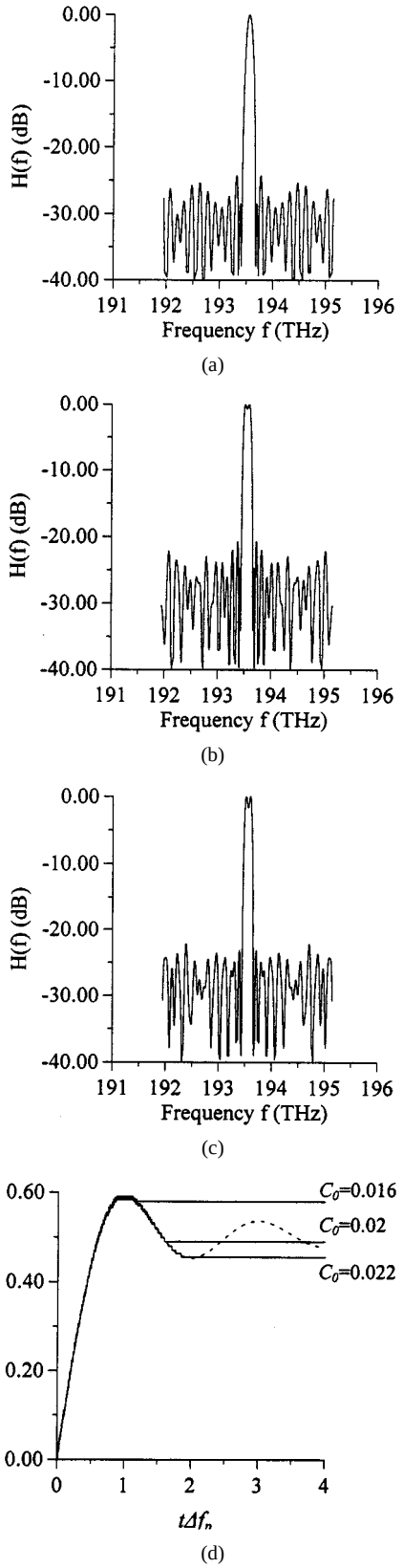

Fig. 4. The normalized transfer function of the tapered AWG for $b = 0.09$ THz and for different values of the initial step C_0. (a) $C_0 = 0.016$. (b) $C_0 = 0.02$. (c) $C_0 = 0.022$. (d) $A(t\Delta f_p)$ (solid lines) and $A_0(t\Delta f_p)$ (dashed line) for the three cases.

$t_m\Delta f_p$ for the case of Fig. 4(b), which practically shows the positions y_m of the grating waveguides [see (24)].

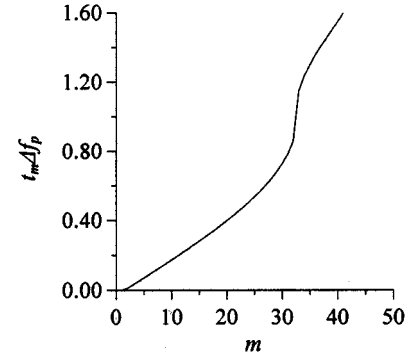

Fig. 5. The variation of $t_m\Delta f_p$ for $C_0 = 0.02$ and $b = 0.09$ THz.

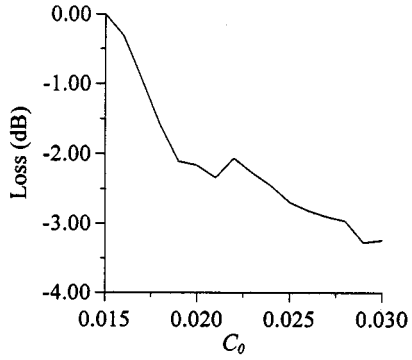

Fig. 6. The variation of loss L_{dB}, defined by (32), as a function of the step C_0 ($b = 0.09$ THz).

B. Design Losses

As discussed before, the deterministic tapering method introduces some losses due to the design itself. In Fig. 4(d), it is shown that some terms $C_m(-1)^{a_m}\cos(2\pi t_m F)$ of the sum in (14) have negative sign at $F = 0$ because of the exponents a_m defined in (12). The losses, which are caused by the negative sign of C_m, depend on C_0. The dependence of the losses with respect to C_0 is depicted in Fig. 6. In the case of Fig. 4(a), the transfer function resembles that of the conventional grating, and most of the terms of the sum in (14) are positive. Consequently, the losses are very low (-0.31 dB). For the cases of Fig. 4(b) and (c), where some of the coefficients are negative, the losses are higher (-2.16 dB and -2.06 dB respectively).

C. The 3-dB Bandwidth

In Fig. 7(a), the dependence of the 3-dB bandwidth on the step C_0 is shown. As C_0 increases, the 3-dB bandwidth quickly reaches 0.14 THz, and after that, it tends slowly to the ideal value of 0.16 THz. In Fig. 7(b)–(d), the normalized transfer functions of the same cases as in Fig. 4(a)–(c) ($C_0 = 0.016, C_0 = 0.02$ and $C_0 = 0.022$) are shown, in the frequency region $[-2\Delta f_p, 2\Delta f_p]$. The dashed lines correspond to the transfer function of an AWG with $C_0 = 0.015$, for which all the terms in (14) are positive at $f = f_0\,(F = 0)$. In Fig. 7(b), the transfer function of a conventional AWG is plotted with heavier dotted lines. It is observed that, even in the case of a transfer function with small C_0 which has only positive terms at $F = 0$, the sidelobes are higher than those of a conventional AWG. This is due to the fact that, although the t_m are nearly

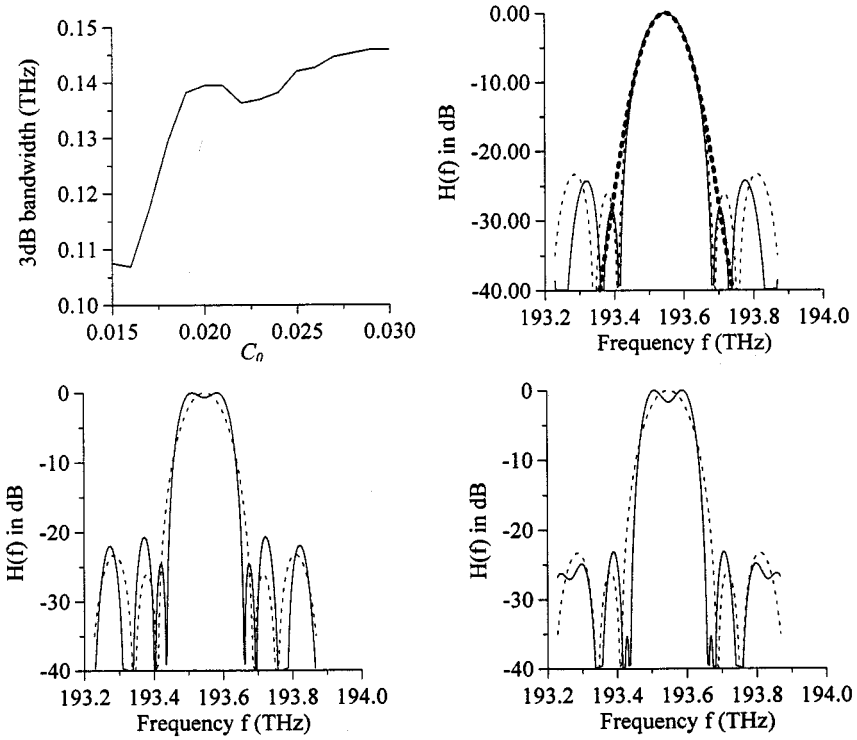

Fig. 7. (a) The 3-dB bandwidth as a function of the initial step C_0. (b) Normalized transfer function of the tapered AWG for the case of Fig. 4(a). The heavier dashed lines represent the transfer function of a conventional AWG. (c) Normalized transfer function of the tapered AWG for the case of Fig. 4(b). (d) Normalized transfer function of the tapered AWG for the case of Fig. 4(c). The transfer function of a tapered AWG with $C_0 = 0.015$ is also shown with dashed lines.

equidistant, as in the conventional AWG, only a portion of the original Gaussian power distribution of the conventional AWG is covered by the C_m. The 3-dB bandwidths of the transfer functions of Fig. 7(b)–(d) are 0.1 THz, 0.139 THz, and 0.136 THz, respectively. It is seen that the flattening of the passband is due to the negative terms, the presence of which results in a better approximation of $A_0(t\Delta f_p)$.

The deterministic tapering technique allows the design of the 3-dB bandwidth of the transfer function simply by adjusting the value of Δf_p and Δf_{ch} and computing the corresponding t_m and C_m. An example is shown in Fig. 8, where the case of Fig. 7(d) has been plotted, along with the transfer function obtained for $\Delta f_p = 0.32$ THz instead of 0.16 THz, $\Delta f_{\text{ch}} = 0.4$ THz instead of 0.2 THz, $b = 0.09$ THz, and $C_0 = 0.0185$. This tapered transfer function has 3-dB bandwidth of 0.272 THz, which is (as Δf_p) twice the 3-dB bandwidth of the case illustrated in Fig. 7(d).

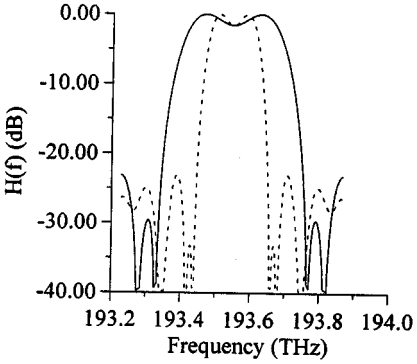

Fig. 8. Two normalized transfer functions designed with different Δf_p. The dashed line represents the design of Fig. 7(d). The solid line represents the design with Δf_p twice that of Fig. 7(d).

D. Reduction of Sidelobe Level

As mentioned previously, the transfer function $H(f)$ can have substantial sidelobes far from the central frequency. One approach in order to reduce the sidelobes is presented.

The transfer function $H(F)$, given by (14), is a sum of P cosine terms, and $1/(2t_m)$ determines the distance between two consecutive zeroes of the mth term. Some of these terms take their maximum values in the vicinity of the positive sidelobes of $H(F)$ and their minimum values in the vicinity of the negative sidelobes. Therefore, the sidelobe level can be improved by omitting these terms from the sum of the transfer function (14). However, some losses can be introduced in the vicinity of the central frequency, and the flatness of the transfer function may also be affected. The number of removed terms must consequently be small (typically two or three out of 41). The terms to be removed are determined numerically in a way to minimize the level of the maximum sidelobe of $H(F)$ without introducing significant losses.

Fig. 9(a) depicts the normalized transfer function obtained for the case of Fig. 4(b), but when the coefficients corresponding to C_0, C_{33} and C_{35} are set equal to zero. The sidelobe level in Fig. 9(a) is -24.3 dB compared to -20.3 dB in Fig. 4(b), whereas the losses introduced by removing the three coefficients is very small (-0.34 dB). This technique can be used to improve the sidelobe levels and can be easily implemented in practice by omitting the waveguides that correspond to the removed terms.

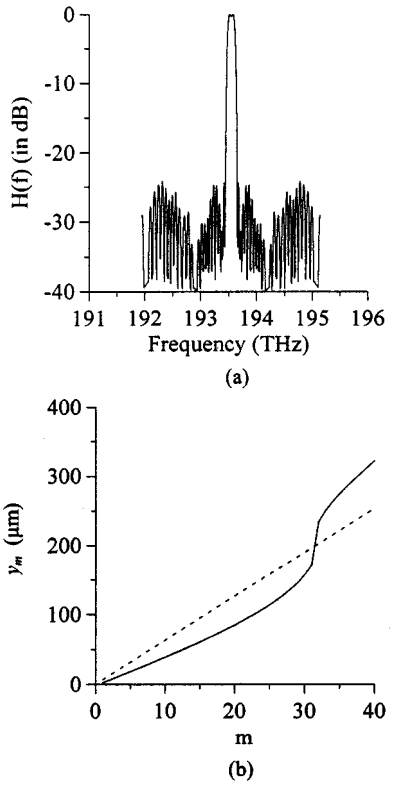

Fig. 9. (a) The normalized transfer function obtained using $C_0 = 0.02, b = 0.09$ THz, and by setting the terms corresponding to C_0, C_{33}, and C_{35} equal to zero. (b) The positions of the grating waveguides y_m for the previous case (solid line) and for an ideal periodic grating with spacing equal to 6.3 μm (dashed line).

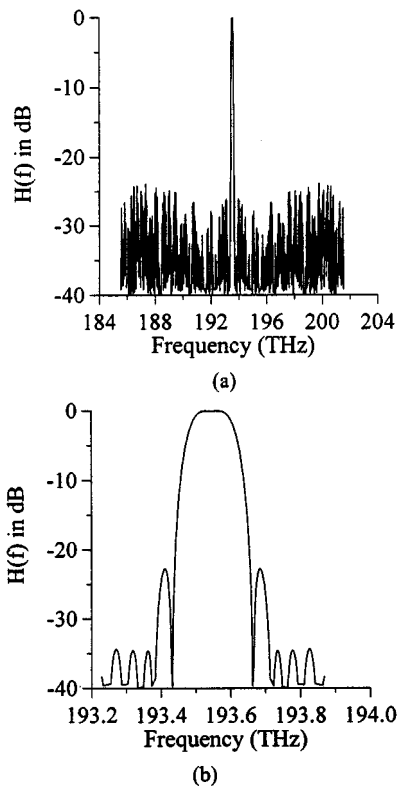

Fig. 10. The normalized transfer function of a flattened AWG with 40 channels. (a) Transfer function in a range of 16 THz around the central frequency $f_0 = 193\ 55$ THz. (b) Transfer function in a region of 0.3 THz around f_0.

E. Coupler Radius and Output Waveguide Spacing

Because of the double chirping technique, the distribution of C_m is related to the distribution of t_m and the constant b, as shown in (26). The value of the constant b, given by (27), is inversely proportional to the spacing Δy_{out} of the output ports (see Fig. 1). Because Δy_{out} cannot be made too small, in order to avoid coupling effects between adjacent output ports, there is a maximum value of b that can be obtained. Coupling can also occur between the grating waveguides. The positions of the centers of the grating waveguides are determined by (24) and (25) and are proportional to the FPR radius R. In order to avoid coupling when the difference between two consecutive t_m is small, R can be adjusted accordingly as in the case of a conventional AWG. Assuming that the length of the core of the waveguides is $d = 2$ μm, that the cores have refractive index equal to $n_w = 3.3$, and that the waveguide index step is $\Delta n_w = 0.02$, then $\sigma \cong 1$ μm. It is, therefore, reasonable to set the center to center spacing of the waveguides at least $\Delta y_{\text{out}} = 4$ μm (Fig. 1(a)). If $\Delta f_{\text{ch}} = 0.2$ THz, then the maximum value of b is found to be $b_{\max} = 0.254$ THz. For the case of Fig. 9(a), where the value of b was set equal to 0.09 THz, the spacing of the output waveguides should be 14 μm. For the case of Fig. 9(a), where the waveguide corresponding to C_0 is omitted, the minimum value $\Delta t_{\min}$ of $t_m - t_{m-1}$ occurs for $m = 2$; that is, $\Delta t_{\min} = t_2 - t_1$, as can be verified from Fig. 2. From (24), we find that the minimum separation between the grating waveguides $\Delta y_{\min}$ is $\Delta y_{\min} = u(t_2 - t_1)$. Requiring that $\Delta y_{\min} = 4$ μm, one finds $u = 32$ for the case of Fig. 9(a). Substituting the value of u in (25) and assuming $n \cong 3.3$, it is found that the coupler radius should be greater than $R_{\min} \cong 4800$ μm. In this way, the minimum radius $R_{\min}$ of the FPR can, in general, be calculated.

F. Position of the Waveguides and Number of Arms

The spacing of the grating waveguides is determined by y_m. For the case of Fig. 9(a), the positions of the grating waveguides is depicted in Fig. 9(b) (solid line), along with those of an ideal periodic grating whose waveguides have center to center distances equal to 6.3 μm (dashed line). The spacing of the ideal grating is chosen so that the difference of the two curves is minimized. As shown in the above figure, there is some deviation of the waveguide positions from those of a perfectly periodic array. The center of the waveguides are positioned 4 μm apart up until the twenty-eighth waveguide, and after that, their spacing increases. This could add insertion loss. This insertion loss can be reduced by a proper choice of the parameters b and C_0 in the initial design and, secondarily, by adding some waveguides where the gap between the waveguides is found to be large. Using the above techniques, the total losses (including the losses, L_{dB}, introduced by the negative terms), compared to those of an ideal AWG, can be kept close to -3 dB.

AWGs with more channels can also be designed using deterministic tapering by employing a larger number of grating arms. The transfer function of a flattened 40-channel AWG is shown in Fig. 10. The number of grating arms is $2P+1 = 201$. The waveguides corresponding to $C_0, C_{78}, C_{91}, C_{92}$, and C_{94} have been excluded in order to reduce the maximum sidelobe at -23 dB.

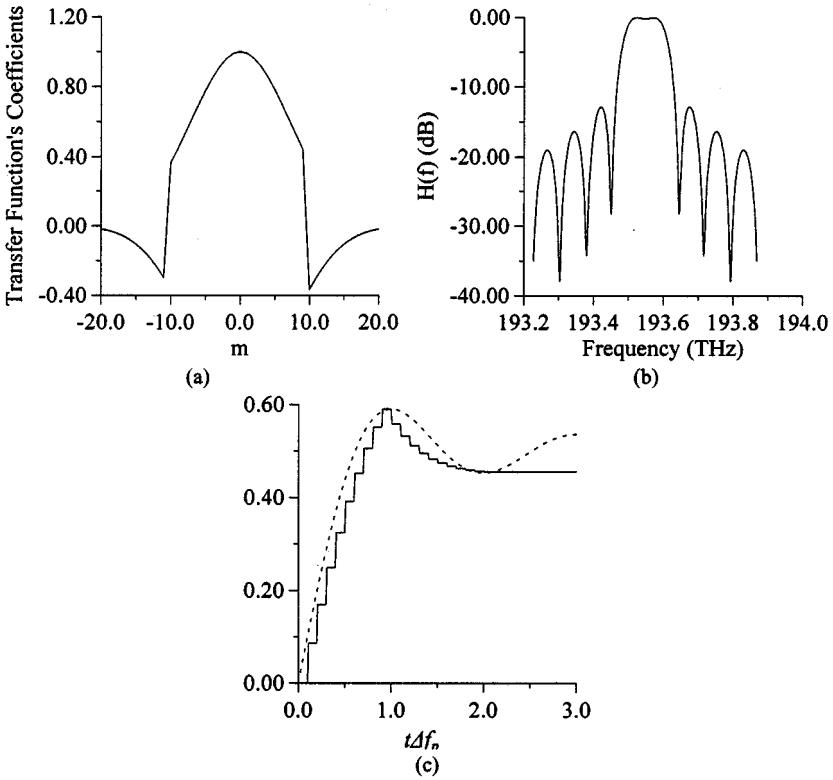

Fig. 11. Design of an AWG transfer function using spatial filtering. (a) The coefficients C_m of the transfer function. (b) The resultant normalized transfer function. (c) The function $A(t\Delta f_p)$ (solid) in comparison with $A_0(t\Delta f_p)$ (dashed).

The increase in number of arms ensures that the sidelobes remain low for a larger frequency range, as compared to the sidelobes of a grating with a smaller number of arms. It should be noted that although there is an increase in the number of arms and, hence, in the number of terms in (14), the maximum sidelobe level has not been reduced. This is because, as discussed in Section III-A, the sidelobe level is caused by other reasons, primarily by the fact that the function $A(t\Delta f_p)$ approximates $A_0(t\Delta f_p)$ only in a finite interval.

IV. Comparison With Other Techniques

For the problem of passband flattening, several solutions have been proposed. Two of them, the spatial filtering and the use of subparabolic chirp, described in [6] and [7], respectively, alter the grating arms as in the proposed method. Spatial filtering is based on the fact that, in the conventional AWG, the transfer function $H(f)$ is the discrete Fourier transform of C_m [3]. In order for $H(f)$ to be approximately rectangular, C_m should resemble a sinc function. This is achieved by making half of the C_m negative, as shown in Fig. 11(a), while the parameters t_m are those of a conventional AWG, given by (6). In Fig. 11(b), the normalized transfer function of [6] is shown. The function $A(t\Delta f_p)$, calculated with the values of C_m and t_m used in [6], has been plotted in Fig. 11(c), where

$$t_m \Delta f_p = \frac{\Delta f_p}{\mathrm{FSR}}\, m. \tag{33}$$

The ideal $A_0(t\Delta f_p)$ is also plotted with a dashed line. It is obvious from Fig. 11(c) that there is some difference between $A(t\Delta f_p)$ and $A_0(t\Delta f_p)$ which is responsible for the high level of sidelobes (higher than 15 dB). This sidelobe level was reduced considerably in [6] by modifying the coefficients C_m in order to achieve smoother transition from the region of positive values to that of negative values. This was achieved by inserting extra losses in the grating waveguides, which has the disadvantage of complicating the design.

Additionally, with this method, the number of waveguides M practically determines the value of Δf_p for a given FSR. Indeed, Δf_p is determined by the first maximum of $A(t\Delta f_p)$. Because $A(t\Delta f_p)$ approximates the function $A_0(t\Delta f_p)$, its first maximum occurs near $t_{\max}\Delta f_p = 1$. This is the point of the last positive C_m, which, from Fig. 11(a), is found to be $C_{M/4}$, corresponding to $t_{M/4}\Delta f_p$. So, $t_{M/4}\Delta f_p = 1$, or using (33) as

$$\Delta f_p = 4\mathrm{FSR}/M. \tag{34}$$

With this particular method, the number of waveguides must be changed in order to change the value of Δf_p, whereas, with the deterministic tapering method, Δf_p can change without affecting the number of waveguides.

Another method, suggested in [7], employs subparabolic chirp in the waveguide lengths. In this method, the t_m are equal to

$$t_m = \frac{1}{\mathrm{FSR}}(m + B|m|^K) \tag{35}$$

where $K \leq 2$. The subparabolic chirp forces the transfer function to broaden. If $C_P \ll C_0$, then the transfer function is approximately Gaussian. In the case where C_P is not negligible,

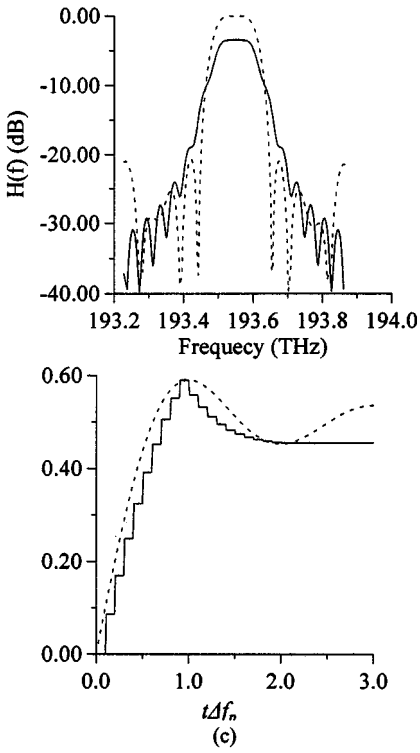

Fig. 12. The transfer function of flattened AWGs using the methods of deterministic tapering (dashed line) and subparabolic chirp (solid line).

the transfer function is a convolution of a sinc and a Gaussian distribution which produces a flatter passband. This technique can produce large 3-dB bandwidths by varying the strength of the chirp B. The flatness depends on the value of K. Their optimal values cannot be computed beforehand, and various cases must be examined. The main feature of this technique is that the passband-to-stopband transition period is larger than that of the proposed technique. Furthermore, the losses introduced are also higher. These are illustrated in Fig. 12, where the normalized transfer function of a flattened AWG is plotted (dashed line) along with the transfer function obtained using the subparabolic chirp technique (solid line) with $M = 41, B = 1.8 \times 10^{-5}$, and $K = 1.90$. The transfer function of the solid line is normalized with respect to the one of the dashed line. The values of K and B are chosen so that the transfer function obtained by the subparabolic chirp technique has minimum ripple and passband equal to the passband of the transfer function obtained by the deterministic tapering technique. The losses inserted due to the first method (solid line) are equal to -6.4 dB. The parameters used in the design procedure of the second method (dashed line) are $b = 0.15, \Delta f_p = 0.16$, and $C_0 = 0.03$, and were chosen in order to decrease the insertion losses. Some waveguides were also added to further decrease the insertion losses, while others were removed in order to decrease the sidelobe level without significantly affecting the 3-dB bandwidth. The total losses of the flattened AWG in the dashed line, compared to an ideal AWG, are -3.1 dB, and the maximum sidelobe level is -21 dB. The total number of waveguides in the array is $M = 81$.

The losses of the subparabolic chirp technique are due to the fact that, with this method, the initial transfer function of a conventional AWG has to broaden in order to become flat, while conserving the energy of the transfer function in the spectral domain, $\int |H(f)|^2 \, df$, as a consequence of Parseval's identity. This forces the peak of the passband to lower. Due to this specific design procedure, the spectral energy of the transfer function is smaller than that obtained using the deterministic tapering method, because, in the latter case, the transfer function is designed to be broad from the beginning. The losses associated with the broadening of the transfer function obtained using the subparabolic chirp technique are -5 dB. There are some additional losses (approximately -1.4 dB), due to the fact that a part of the incident beam at the first star coupler is not intercepted by any grating waveguides (because C_P must not be too small compared to C_0). It should also be noted the distribution of (35) may not be optimal, in the sense that other distributions may produce better results.

V. Conclusion

A novel method for shaping the transfer function of an AWG has been described. The method reduces the optimization of the transfer function to the problem of adjusting the waveguide lengths in order to minimize a certain error function. It uses simple mathematical formulas and is not based on empirical rules. In order to achieve the same passband on each output port, the positions of the grating waveguides on the edge of the FPRs is also adjusted. The technique does not require a large number of waveguides, results in low values of sidelobe level, and can easily be used to design transfer functions with a given 3-dB bandwidth. It should also be noted that, using this technique, one can also shape the transfer function in a form other than rectangular by modifying the function to be approximated.

References

[1] C. A. Brackett, "Dense wavelength division multiplexing networks: Principles and applications," *IEEE J. Select. Areas Commun.*, vol. 8, pp. 948–964, June 1990.

[2] C. Dragone, "An $N \times N$ optical multiplexer using a planar arrangement of two star couplers," *IEEE Photon. Technol. Lett.*, vol. 3, pp. 812–815, Sept. 1991.

[3] K. Okamoto and H. Yamada, "Arrayed waveguide grating multiplexer with flat response," *Opt. Lett.*, vol. 20, pp. 43–45, Jan. 1995.

[4] M. R. Amersfoort, J. B. D. Soole, H. P. LeBlance, N. C. Andreadakis, A. Rajhel, and C. Caneau, "Passband broadening of integrated arrayed waveguide filters using multimode interference couplers," *Electron. Lett.*, vol. 23, pp. 449–451, 1996.

[5] Y. P. Ho, H. Li, and Y. Chen, "Flat channel passband wavelength multiplexing and demultiplexing devices by multiple rowland circle design," *IEEE Photon. Technol. Lett.*, vol. 9, pp. 342–344, Mar. 1997.

[6] C. Dragone, T. Strasser, G. A. Bogert, L. W. Stulz, and P. Chou, "Waveguide grating router with maximally flat channel passband produced by spatial filtering," *Electron. Lett.*, vol. 33, no. 15, pp. 1312–1314, July 1997.

[7] M. C. Parker and S. D. Walker, "Design of arrayed waveguide gratings using hybrid fourier-fresnel transfom techniques," *IEEE J. Select. Areas Quantum. Electron.*, vol. 5, pp. 1379–1384, Sept./Oct. 1999.

[8] R. E. Collin and F. J. Zucker, *Antenna Theory Part I*. New York: McGraw-Hill, 1969, pp. 212–219.

[9] A. W. Snyder and J. D. Love, *Optical Waveguide Theory*. London, U.K.: Chapman & Hall, 1983.

[10] C. R. Doerr and C. H. Joyner, "Double chirping of the waveguide grating router," *IEEE Photon Technol. Lett.*, vol. 9, June 1997.

[11] P. M. Morse and H. Feshbach, *Methods of Theoretical Physics Part I*. New York: McGraw-Hill, 1953, p. 456.

Thomas Kamalakis was born in Athens, Greece, on September 1, 1975. He received the B.S. degree in informatics and the M.Sc. degree in telecommunications from the University of Athens, Athens, Greece, in 1997 and 1999, respectively. He is currently pursuing the Ph.D. degree, working on the design and modeling of arrayed waveguide gratings.

Thomas Sphicopoulos (M'87) received the degree in physics from the University of Athens, Athens, Greece, in 1976, the D.E.A. and Doctorate degrees in electronics from the University of Paris VI, Paris, France, in 1977 and 1980, respectively, and the Doctorat Es Science degree from the Ecole Polytechnic Federal de Lausanne (EPFL), Lausanne, Switzerland, in 1986.

From 1977 to 1980, he was with Thomson-CSF, and in 1980, he joined the Electromagnetic Laboratory of EPFL. Since 1980, he has been with the Optical Communications Laboratory of the University of Athens. He is currently a Professor of Informatics at the university. He has authored or coauthored approximately 70 scientific papers in the fields of telecommunications and optical communications. He has participated in a number of European and Greek projects, and he has been an auditor and evaluator of RACE and ACTS projects. He is an adviser in several organizations, including EETT (Greek NRA for telecommunications).